Journal of the Optical Society of Korea
Vol. 14, No. 1, March 2010, pp. 28-32

DOI: 10.3807/JOSK.2010.14.1.028

Spectrally Phase Coded Waveform Discrimination at 10 GHz for Narrow Band Optical CDMA within 100 GHz Spectral Window

Dong-Sun Seo*

Department of Electronic Engineering, Myongji University, Yongin 449-728, Korea

V. R. Supradeepa

Department of Electrical Engineering, Purdue University, West Lafayette, IN 47906, USA

(Received September 22, 2009 : revised December 17, 2009 : accepted January 5, 2010)

We demonstrate binary spectral phase coded waveform discrimination at 10 GHz for narrow band optical code-division multiple-access (NB-OCDMA) via direct electrical detection without using any optical hard-limiter. Only 9 phase-locked, 10 GHz spaced, spectral lines within a 100 GHz spectral window are used for the phase coding. Considerably high contrast ratio of 5 between signal and multiuser access interference noise can be achieved for 4 × 10 G pulse/sec timing coordinated OCDMA at a simple electrical receiver with 50 GHz bandwidth.

Keywords : Optical code-division multiple-access (OCDMA), Spectral phase coding, Pulse shaping, Spectral efficiency
OCIS codes : (060.4510) Optical communications; (320.5540) Pulse shaping; (060.4250) Networks

I. INTRODUCTION

Optical code-division multiple-access (OCDMA) is receiving increased attention due to its potential to enhance information security, simplify and decentralize network control, improve spectral efficiency, and increase flexibility in the granularity of bandwidth that can be provided [1-4]. However, for practical applications, there are several issues to overcome, including low spectral efficiency, large multiuser access interference (MAI) as well as others. Spectrally phase coded OCDMA has been studied in detail [4-7] and attempts have been made to overcome these problems. In spectrally phase coded OCDMA, a mode-locked laser produces phase-locked spectral lines, evenly spaced with the pulse repetition rate. These lines are coded by a pseudo-random phase modulation. The random phase coding disturbs the phase-locked feature and spreads the pulse in time, converting the input short pulses into noise like, low intensity signals. In a receiver, the same coder is used to recover the original phase, and the noise-like signal is converted back to the original pulse signal, while waveforms from other users (*i.e.*, MAI noise) which use different codes retain phase-disturbed, low-intensity, noise-like waveforms, which are very similar to the coded signals [4-7]. This means that decoding of a random phase coded waveform simply returns to a random coded waveform set unless the decoding is matched to the pulse. Similar characteristics of the spectrally phase coded OCDMA have been used also for code translation [8]. Therefore, the contrast ratio between the (matched) target signal and (unmatched) MAI noise, which is a measure of system performance, can be simply determined by the ratio between the input pulse and the coded waveforms [9]. To increase this ratio, a large number of spectral chips is required. Results of greater than 20 dB contrast ratio have been obtained by spectral phase coding of ultrashort pulses (broad band with bandwidth W) [4, 5, 9]. Having a high contrast ratio enables us to increase the total number of users (N), enhancing the spectral efficiency. However, too many users in a single channel induce system performance degradation due to overlap between multiuser signals in the time domain [5]. To reduce this degradation we can divide the wide spectral band W into M narrow band (with the spectral window $B = W/M$) spectral groups. Then we implement L user OCDMA for each narrow band

*Corresponding author: sdsphoto@mju.ac.kr

Color versions of one or more of the figures in this paper are available online.

(NB) spectral group, introducing a potential for wavelength division multiplexing (WDM) of OCDMA channel groups. Small (but greater than N/M) user number L can reduce the probability of user signal overlap in time and increase the spectral efficiency. For example, a 20×10 Gb/s (N=20) broad band (BB) OCDMA system with W=16 nm can be divided into 20 channel groups (M=20) of 4×10 Gb/s (L=4) NB-OCDMA systems with B=0.8 nm. The probability of the signal overlap at the above NB-OCDMA receiver can be reduced up to 1/5, whereas the spectral efficiency can increase up to 4 times, compared with those of a BB-OCDMA. Recently, Etemad *et al.* studied this NB-OCDMA, where 16 spectral lines within the 80 GHz bandwidth were coded for 4×2.5 Gb/s and 6×5 Gb/s OCDMA systems, and they achieved spectral efficiencies of 0.125 bit/Hz and 0.375 bit/Hz respectively [6, 7]. However, the relatively good efficiency of 0.375 bit/s in [7] was achieved by an additional polarization multiplexing, which reduces the significance of the value to half (0.1875 bit/s). Further improvement of the spectral efficiency can be achieved by reducing the number of spectral lines while increasing the speed of each OCDMA channel, and by multiplexing with a signal which has other modulation formats. For example, we can imagine a WDM/OCDMA hybrid transmission, whose spectral allocation is schematically shown in Fig. 1. The OCDMA channels can be implemented by passing mode-locked short pulses through an arrayed waveguide grating (AWG), while the WDM channels are implemented by passing through a high finesse Fabry-Perot interferometer. In practice, ITU DWDM signals with 100 GHz spacing and multichannel NB-OCDMA signals within 100 GHz spectral window groups can be transmitted together through a single fiber.

In this work, as a preliminary study of our idea, we will use 9 spectral lines spaced at 10 GHz (*i.e.*, pulse repetition frequency f_{rep}=10 GHz) within a 100 GHz spectral window, ensuring compatibility with conventional ITU DWDM networks, and we will show successful spectrally phase coded waveform discrimination for 4 user 10 G pulse/sec OCDMA. Our NB-OCDMA itself (without polarization multiplexing and/or hybrid transmission with DWDM) has a potential spectral efficiency of 0.4 bit/Hz (3.2 times of [6]). Due to narrow bandwidth, the number of available spectral chips becomes small and a relatively low contrast ratio between the signal and MAI noise is expected. To optimize this contrast ratio, we need to maximize the number of spectral chips, and this we do by setting the individual spectral chips matched one-to-one with individual spectral lines, allowing spectral line-by-line coding of 9 spectral lines. Note that both coded and uncoded waveforms repeat with period T=1/f_{rep}, but a random phase coded waveform spans the full time period T while the uncoded pulse is isolated in time. Here we expect uncoded signal pulses with ~10 ps temporal and ~50 GHz spectral widths within a 100 GHz spectral window. The narrow spectral width, leading to a relatively broad signal pulse, allows us to use a simple electrical threshold based on a photo-detector for signal discrimination from MAI noise, without the need for a nonlinear optical hard-limiter where the second harmonic MAI noise is enhanced due to overlap between the signal and MAI waveforms [5]. Therefore, our NB-OCDMA has a distinct advantage at the receiver in addition to its high spectral efficiency.

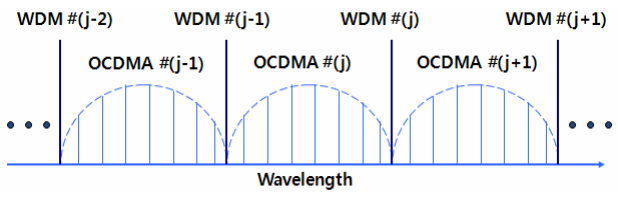

FIG. 1. WDM and OCDMA spectral allocation for WDM/OCDMA hybrid transmission.

II. EXPERIMENTAL SETUP

To spread the coded waveform to be as broad and flat as possible within the time period T, we need to manipulate independently the phase of the 9 individual spectral lines (line-by-line spectral phase coding). For the line-by-line spectral phase coding, we build a well-known Fourier Transform pulse shaper coder [5, 10] based on a liquid crystal modulator (LCM) array with 128 pixels of 100 ㎛ each, as shown in Fig. 2. The individual pixels can be electrically controlled to give a random phase shift and intensity modulation. Even though the phase modulation is enough for our OCDMA coding, the intensity modulation is also applied to prepare a NB-OCDMA pulse source with ~50 GHz bandwidth within a 100 GHz spectral window. The OCDMA coder has a reflective geometry where input and output are separated via an optical circulator. A polarization controller

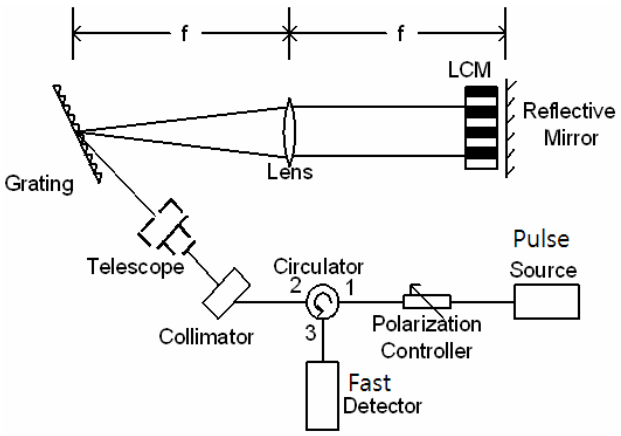

FIG. 2. Experimental set-up for NB-OCDMA spectral phase coding of individual spectral lines. Individual LCM pixels independently control both phase and intensity of the spectral lines spaced at 10 GHz.

(PC) is used to get maximum diffraction performance at the 1200 grooves/mm diffractive grating. Since the spectral resolving power of the grating is proportional to the size of the beam spot on it, a fiber pigtailed collimator and subsequent telescope magnify the input beam size to 16-mm diameter. Discrete spectral lines of the input short pulse are diffracted by the grating and focused by the lens with 1-m focal length. The LCM array placed just before the focal plane independently controls both intensity and phase of the spectral components falling on the LCM. A retro-reflecting mirror returns the modulated spectral lines to a fiber, allowing them to exit through an optical circulator.

From the Fourier transform configuration, we can easily arrive at the following relationship between the wavelength ($\Delta\lambda$) and the spatial (Δx) separations for the first order diffracted light.

$$\frac{\Delta\lambda}{\Delta x} = \frac{d\cos\theta_d}{f} \tag{1}$$

where d is the grating constant, θ_d the grating diffraction angle, and f the lens focal length.

We adjusted the diffracted (*i.e.*, incident) beam angle of the coder at ~62° (corresponding incident angle of ~76°) to minimize crosstalk due to the spot size and also to the nonideal spot shape on the Fourier plane. Then each line spaced at 10 GHz in 1.55 ㎛ occupies 2 pixels of 100 ㎛ each, leading to line to line spacing of 200 ㎛.

Now we can get the beam radius w_0 of the coder at the LCM (*i.e.*, focal) plan as follows,

$$w_0 = \frac{\lambda f\cos\theta_i}{\pi w_i\cos\theta_d} \tag{2}$$

where λ is the wavelength, θ_i the grating incident angle, and w_i the incident beam radius.

The spectral resolution of the coder can be defined as the spectral width corresponding to beam diameter $2w_0$. Our system shows the focused beam diameter of ~65 ㎛, corresponding to the spectral resolution of ~3 GHz, which is high enough to control accurately the phase and intensity of individual spectral lines spaced at 10 GHz. Finally, the temporal waveforms and optical spectra are measured by a fast 50 GHz sampling scope coupled with a fast (60 GHz) photo-detector and an optical spectral analyzer with 0.01 nm resolution, respectively.

III. EXPERIMENTAL RESULTS AND DISCUSSION

To select 9 phase locked spectral lines within a 100 GHz spectral window from a frequency comb constituting of short pulses at 10 GHz repetition rate, we program the pixels of the LCM in Fig. 2 such that 9 lines are allowed and the rest are blocked. The intensity of the allowed spectral lines is adjusted to imitate an AWG-passed envelope (*i.e.*, an OCDMA channel in Fig. 1). Fig. 3 shows the optical spectrum and sampling scope trace of the pulse source prepared for our NB-OCDMA coding. Only 9 spectral lines within a 100 GHz spectral window and their AWG-passed like intensity envelope are shown in Fig. 3(a). Due to the limited bandwidth (50 GHz) of our measurement system the pulse width is slightly broadened from 10 ps to 15 ps, but most of its power is well confined within a narrow time interval of ~20 ps within the period of 100 ps, as shown in Fig. 3(b). This indicates that an electrical receiver with a commercially available 50 GHz photo-detector will be good enough for the suggested NB-OCDMA to discriminate the signal from MAI noise, as long as the MAI noise waveforms spread well within the time period. After the intensity adjustment, the individual spectral lines are coded by pseudorandom binary phase.

Here we emulate a 4 user OCDMA system; an uncoded pulse signal and 3 of coded MAIs. To form the MAI waveforms, we apply pseudorandom binary phase shift for each of the 9 spectral lines (or chips) as follows; code #1

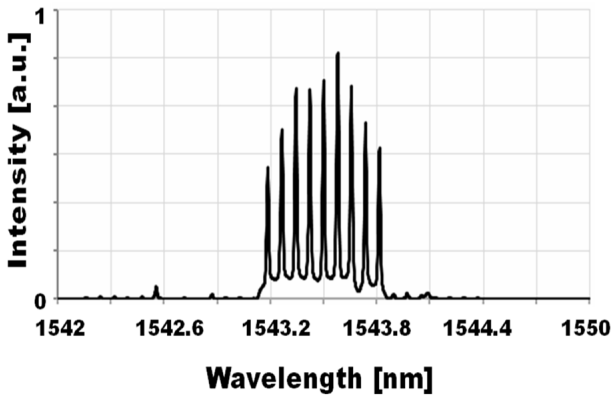

(a)

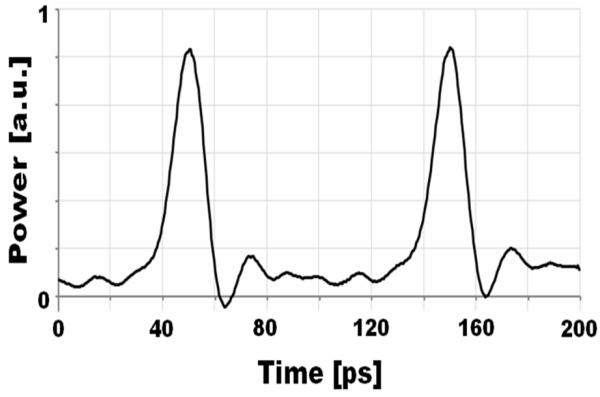

(b)

FIG. 3. The pulse source prepared for our NB-OCDMA; (a) optical spectrum showing 9 spectral lines within a 100 GHz spectral window, and (b) temporal trace showing well isolated pulses within the 100 ps period.

= [0, π, π, 0, 0, 0, 0, π, π], code #2 = [0, π, 0, 0, π, π, 0, 0, π], and code #3 = [0, π, 0, 0, π, 0, π, π, 0]. Since the phase shift does not affect the intensity, no noticeable change in optical spectra is observed. However, temporal MAI waveforms (measured by a 50 GHz sampling scope) change dramatically, as shown in Fig. 4. To show the waveforms in detail we trace individual waveforms for a single period (100 ps). Individual coded MAI waveforms spread differently in time but show similar low intensity characteristics to be easily discriminated from the target pulse signal shown in Fig. 3(b).

To examine the worst case where all MAI waveforms exist, we compare the uncoded pulse signal with the sum of 3 coded MAI waveforms, as shown in Fig. 5 (no interference between the signal and/or MAI waveforms was assumed). Unfortunately, Fig. 5 shows that asynchronous detection may not be applicable for the NB-OCDMA, since the peak signal to MAI ratio becomes very poor depending on timing of individual MAI waveforms. However, if we use time coordinated synchronous detection [11] at the original pulse position (around time t=48 ps in Fig. 5), we can achieve the signal to MAI ratio of ~5, which is enough for electrical discrimination of the signal from MAI noise.

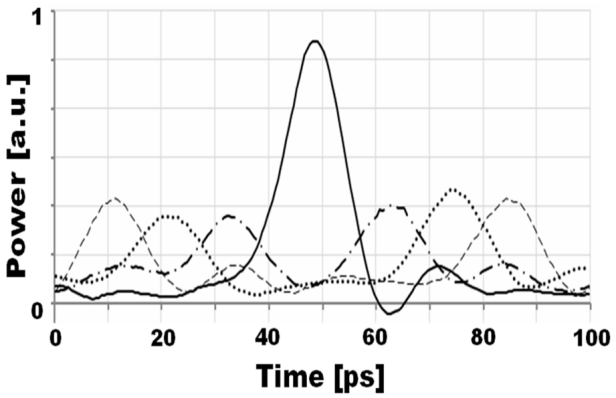

FIG. 4. Temporal waveforms measured by a 50 GHz sampling scope coupled width a fast detector; solid line – uncoded (pulse signal), dash-dotted line – coded by the code #1, dotted line – coded by the code #2, and dashed line – coded by the code #3. The waveforms repeat with the 100 ps (= 1/10 GHz) period.

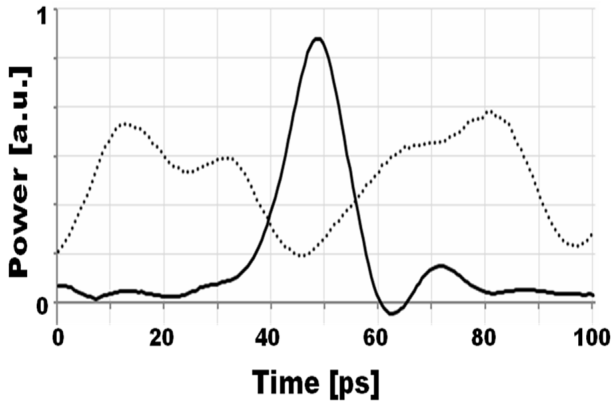

FIG. 5. Comparison of target pulse signal (solid line) and the sum of 3 MAI waveforms (dotted line). No interference between the signal and/or MAI waveforms was assumed.

To confirm our result through simulation using a photonics simulation package, we generate 9 phase-locked spectral lines corresponding to those in Fig. 3 and perform binary phase coding based on the codes given in the experiment. Fig. 6 shows pulse signal and coded MAI waveforms. Here we assumed an ideal binary phase coder and a 50 GHz photo-detector. Note that the waveforms, especially those which are time spread by the phase coding, are very similar to those of the experiment. Slight differences in the waveforms may be caused by non-ideal devices used in the experiment. The peak signal to total MAI noise ratio becomes similar to that of the experiment, while the signal to MAI ratio at the original pulse position (t=50 ps) is much higher than in the experiment, approaching 30. Actually we selected the phase codes such that all coded waveforms spread out perfectly from the original position by splitting to both sides. However, the waveform coded by code #1 has too small a gap between its split pulses, causing the photo-detector with limited bandwidth to show power fill up between the pulses, as shown by the dash-dotted line in Fig. 6. Note that even a small timing (or delay) difference in the spread waveforms gives a big change in the ratio at t=50 ps. This indicates further improvement of the ratio in the experiment would be possible.

Next we apply pseudorandom pulse modulation for the 4 user 10 Gb/s NB-OCDMA and examine its eye diagram, as shown in Fig. 7. Again we ignore the interference between the pulse signal and/or MAI waveforms, and assume a time coordinated synchronous detection in the receiver. Clear eye-opening is observed around the original pulse position, as expected in Fig. 6.

The good agreement between the experiment and simulation

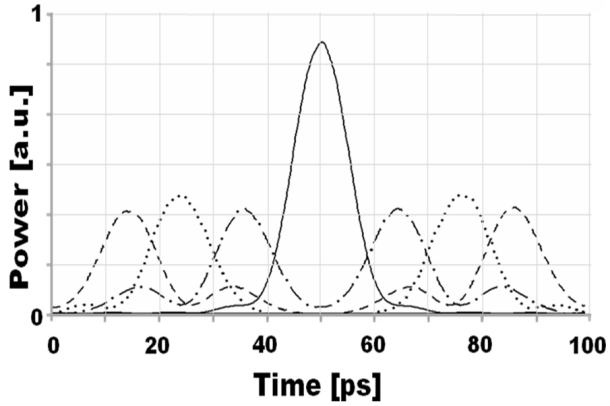

FIG. 6. Simulated waveforms of uncoded pulse signal (solid line) and coded MAI waveforms (dash-dotted line – code #1, dotted line – code #2, and dashed line – code #3), corresponding to those in Fig. 4.

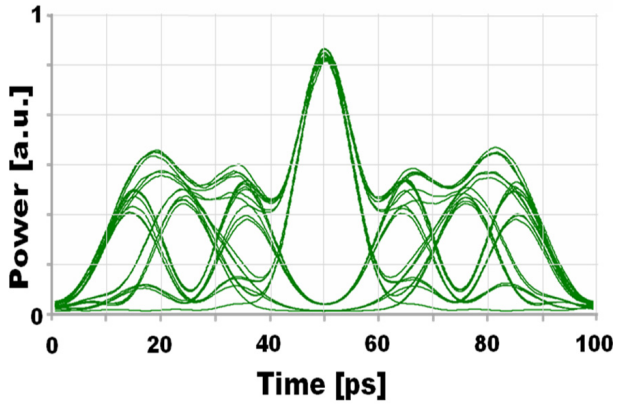

FIG. 7. Simulated eye diagram at the time coordinated synchronous receiver for our 4 x 10 Gb/s NB-OCDMA.

enables us to examine the performance of various spectral phase coding algorithms for a given number of spectral lines through simulation (without experiment) and to find an optimum code family with maximum temporal spread but minimum overlap among users.

IV. CONCLUSION

We performed a feasibility study of NB-OCDMA which has a potential for high spectral efficiency by allowing a larger number of users and by providing compatibility with conventional ITU DWDM networks. For OCDMA phase coding we built a high resolution line-by-line spectral coder with ~3 GHz of spectral resolution, which is capable of controlling accurately the phase and intensity of individual spectral lines with 10 GHz spacing. Based on the line-by-line coder, only 9 phase-locked, 10 GHz spaced, spectral lines within a 100 GHz spectral window (corresponding to the ITU DWDM channel spacing) were prepared for our NB-OCDMA from a 10 GHz short pulse source. Next we applied pseudorandom binary phase on the prepared spectrum to generate 3 MAI waveforms. For the uncoded pulse signal discrimination from the MAI noise, we used a simple electrical receiver (~50 GHz bandwidth) with a commercially available fast photo-detector. Even thought an asynchronous receiver might not be applicable to our NB-OCDMA, considerably high contrast ratio of ~5 between the target signal and MAI noise could be achieved at the time coordinated synchronous receiver. Further improvement in the contrast ratio would be possible by more deliberate phase control of the spectral lines. Simulations using a photonics package agreed well with the experiments, proving the validity of the suggested idea. In this way, we demonstrated binary spectral phase coded waveform discrimination for 4×10 G pulse/sec NB-OCDMA via direct electrical detection. Potential spectral efficiency of the suggested system was 0.4 bit/Hz and would increase up to 1 bit/Hz by polarization multiplexing and hybrid transmission with ITU DWDM signals.

ACKNOWLEDGMENT

This work was supported by the Korea Research Foundation (#2009-0072630). We thank Prof. A. M. Weiner for the use of the Purdue University Ultrafast Optics and Fiber Communications Laboratory and for his comments, and thank Mr. I. W. Kim for his help in preparing the modified manuscript.

REFERENCES

1. J. E. McGeehan, S. M. Reza, M. Nezam, P. Saghari, A. E. Willner, R. Omrani, and P. V. Kumar, "Experimental demonstration of OCDMA transmission using a three-dimensional (time-wavelength-polarization) codeset," IEEE J. Lightwave Technol. **23**, 3282-3289 (2005).
2. H. Stobayashi, W. Chujo, and K. Kitayama, "Highly spectral-efficient optical code-division multiplexing transmission systems," IEEE J. Select. Topics Quantum Electron. **10**, 250-258 (2004).
3. S. C. Kim, S. Y. Shin, and D. S. Seo, "Design and performance analysis of 2-dimensional optical CDMA encoder/decoder using an array of SSFBGs," J. Opt. Soc. Korea **9**, 95-98 (2005).
4. W. Cong, C. Yang, R. P. Scott, V. J. Hernandez, N. K. Fontaine, B. H. Kolner, J. P. Heritage, and S. J. B. You, "Demonstarion of 160- and 320-Gb/s SPECTS O-CDMA network testbeds," IEEE Photon. Technol. Lett. **18**, 1567-1569 (2006).
5. A. M. Weiner, Z. Jiang, and D. Lieard, "Spectrally phase-coded O-CDMA," J. Opt. Net. **6**, 728-755 (2007).
6. S. Etemad, P. Toliver, R. Menendez, J. Young, T. Banwell, S. Galli, J. Jackel, P. Delfyett, C. Price, and T. Turpin, "Spectrally efficient CDMA using coherent phase-frequency coding," IEEE Photon. Technol. Lett. **17**, 929-931 (2005).
7. A. Agrawal, P. Toliver, R. Menendez, T. Banwell, J. Jackel, and S. Etemad, "Spectrally efficient six-user coherent OCDMA system using reconfigurable integrated ring resonator circuits," IEEE Photon. Technol. Lett. **18**, 1952-1953 (2006).
8. D. S. Seo, Z. Jiang, D. E. Leaird, and A. M. Weiner, "Pulse shaper in a loop: demonstration of cascadable ultrafast all-optical code-translation," Opt. Lett. **29**, 1864-1866 (2004).
9. Z. Jiang, D. S. Seo, S.-D. Yang, D. E. Leaird, R. V. Roussev, C. Langrock, M. M. Fejer, and A. M. Weiner, "Low power, high-contrast coded waveform discrimination at 10 GHz via nonlinear processing," IEEE Photon. Technol. Lett. **16**, 1778-1780 (2004).
10. Z. Jiang, D. E. Leaird, and A. M. Weiner, "Optical processing based on spectral line-by-line pulse shaping on a phase-modulated CW laser," IEEE J. Quantum Electron. **42**, 657-666 (2006).
11. Z. Jiang, D. S. Seo, D. E. Leaird, A. M. Weiner, R. V. Roussev, C. Langrock, and M. M. Fejer, "Multi-user, 10 Gb/s spectrally phase coded O-CDMA system with hybrid chip and slot-level timing coordination," IEICE Electron. Exp. **1**, 398-403 (2004).